

Supplementary Information for:

Reversible Methanol Addition to Copper Schiff Base Complexes: A Kinetic, Structural, and Spectroscopic Study of Reactions at Azomethine C=N Bonds

Wuyu Zhang,^a Nina Saraei,^a Hanlin Nie,^a John R. Vaughn,^a Alexis S. Jones,^a Mark S. Mashuta,^a Robert M. Buchanan,^a and Craig A. Grapperhaus^{*a}

^aDepartment of Chemistry, University of Louisville, 2320 South Brook Street, Louisville, KY, USA 40292.
e-mail: grapperhaus@louisville.edu

Contents

Crystallographic Methods.....	3
References.....	5
Table S1. Crystal Data and Structure Refinement for 1,4 – 7 , and L ₁	6
Figure S1. Electronic spectrum of 2 in acetonitrile.	7
Figure S2. Electronic spectrum of 3 in acetonitrile.	7
Figure S3. Electronic spectrum of 6 in acetonitrile.	8
Figure S4. Electronic spectrum of 7 in acetonitrile.	8
Figure S5. Electronic spectrum of 8 in acetonitrile (non-dried).	9
Figure S6. IR spectrum of 1	10
Figure S7. IR spectrum of 2	10
Figure S8. IR spectrum of 3	11
Figure S9. IR spectrum of 4	12
Figure S10. IR spectrum of 5	12
Figure S11. IR spectrum of 6	13
Figure S12. IR spectrum of 7	13
Figure S13. +ESI spectrum of 1	14
Figure S14. +ESI spectrum of 2	15
Figure S15. +ESI spectrum of 3	16
Figure S16. +ESI spectrum of 4	17
Figure S17. +ESI spectrum of 5	18
Figure S18. +ESI spectrum of 6	19

Figure S19. +ESI spectrum of 7 .	19
Figure S20. Experimental and simulated room temperature powder EPR spectrum of 1 .	20
Figure S21. Experimental and simulated room temperature powder EPR spectrum of 5 . The small feature near B = 3500 G is an impurity in the EPR tube.	21
Figure S22. ORTEP ⁴ representation of {[L ₂ -Cu(CH ₃ OH)]·OTf} ⁺ of 6 .	21
Figure S23. ORTEP ⁴ representation of [L ₂ -Cu(CH ₃ OH)] ²⁺ of 7 .	22
Figure S24. Non-covalent interactions in 6 . Hydrogen bond D···A acceptor distances are indicated in units of Å.	22
Figure S25. Non-covalent interactions in 7 . Hydrogen bond D···A acceptor distances are indicated in units of Å.	23
Figure S26. Plot of <i>k_{obs}</i> versus [CH ₃ OH] for 1 and 4 .	24
Figure S27. Plot of <i>k_{obs}</i> versus [CH ₃ OH] for 2 and 3 .	24

Crystallographic Methods

A blue plate 0.42 x 0.40 x 0.03 mm³ crystal of **1** grown from a solution of dry acetonitrile/ether was mounted on a glass fiber for collection of x-ray data on an Agilent Technologies/Oxford Diffraction Gemini CCD diffractometer. The CrysAlisPro¹ CCD software package (v 1.171.36.32) was used to acquire a total of 1,521 fifteen-second frame ω -scan exposures of data at 100K to a $2\theta_{\max} = 57.40^\circ$ using monochromated MoK α radiation (0.71073 Å) from a sealed tube. Frame data were processed using CrysAlisPro¹ RED to determine final unit cell parameters: $a = 8.7479(8)$ Å, $b = 10.1421(7)$ Å, $c = 12.9690(10)$ Å, $\alpha = 68.941(7)^\circ$, $\beta = 75.950(7)^\circ$, $\gamma = 88.025(7)^\circ$, $V = 1039.90(14)$ Å³, $D_{\text{calc}} = 1.749$ Mg/m³, $Z = 2$ to produce raw hkl data that were then corrected for absorption (transmission min./max. = 0.627 /1.000; $\mu = 1.367$ mm⁻¹) using SCALE3 ABSPACK². The structure was solved by Direct methods in the space group P1bar using SHELXS-90³ and refined by least squares methods on F^2 using SHELXL-97³. Non-hydrogen atoms were refined with anisotropic atomic displacement parameters. Methylene, methine and imidazole hydrogen atoms were located by difference maps and refined isotropically. Methyl hydrogen atoms were placed in their geometrically generated positions and refined as a riding model and these atoms were assigned $U(\text{H}) = 1.5 \times U_{\text{eq}}$. For all 5,359 unique reflections ($R(\text{int})$ 0.049) the final anisotropic full matrix least-squares refinement on F^2 for 332 variables converged at $R1 = 0.038$ and $wR2 = 0.089$ with a GOF of 1.04.

Crystals of **4** suitable for x-ray analysis were grown from a non-dried acetonitrile/ether solution and mounted on a CryoLoop for collection of x-ray data on an Agilent Technologies/Oxford Diffraction Gemini CCD diffractometer. X-ray structural analysis for **4** was performed on a 0.28 x 0.21 x 0.02 mm³ blue plate using a 835 frame, forty second frame ω -scan data collection strategy at 100 K to a $2\theta_{\max} = 55.50^\circ$. Complex **4** crystallizes in the triclinic space group P-1 with unit cell parameters: $a = 8.227(3)$ Å, $b = 11.003(4)$ Å, $c = 11.441(4)$ Å, $\alpha = 78.99(3)^\circ$, $\beta = 70.69(3)^\circ$, $\gamma = 88.76(3)^\circ$, $V = 958.4(6)$ Å³, $Z = 2$ and $D_{\text{calc}} = 1.818$ Mg/m³. 4,447 independent data were corrected for absorption (transmission min./max. = 0.038 /1.000; $\mu = 1.481$ mm⁻¹). The structure was solved by Direct methods using SHELX³. All non-hydrogen atoms were refined with anisotropic atomic displacement parameters. Hydrogen atoms were located and refined as described above for **1**. For reflections $I > 2\sigma(I)$ ($R(\text{int})$ 0.043) the final anisotropic full matrix least-squares refinement on F^2 for 317 variables converged at $R1 = 0.054$ and $wR2 = 0.127$ with a GOF of 1.06.

Crystals of **5** were grown from a methanol/ether solution and mounted on a glass fiber for collection of x-ray data on an Agilent Technologies/Oxford Diffraction Gemini CCD diffractometer. X-ray structural analysis for **5** was performed on a 0.35 x 0.28 x 0.26 mm³ blue prism using a 1,337 frame, twenty second frame ω -scan data collection strategy at 100 K to a $2\theta_{\max} = 56.3^\circ$. Complex **5** crystallizes in the monoclinic space group Pn with unit cell parameters: $a = 13.0049(3)$ Å, $b = 11.5913(2)$ Å, $c =$

15.1039(4) Å, $\beta = 104.371(3)^\circ$, $V = 2205.57(9) \text{ \AA}^3$, $Z = 4$ and $D_{\text{calc}} = 1.719 \text{ Mg/m}^3$. The 10,813 independent data were corrected for absorption (transmission min./max. = 0.808 /1.000; $\mu = 1.298 \text{ mm}^{-1}$). The structure was solved by Patterson methods using SHELX³ and contains two molecules in the asymmetric unit. All non-hydrogen atoms were refined with anisotropic atomic displacement parameters. Amine NH's and methanol OH's were located by difference maps and refined isotropically. Methylene, methine, imidazole and methyl hydrogen atoms were placed in their geometrically generated positions, refined as riding models and these atoms were assigned $U(\text{H}) = 1.2, 1.2, 1.2$ and $1.5 \times U_{\text{eq}}$ respectively. For reflections $I > 2\sigma(I)$ ($R(\text{int}) 0.041$) the final anisotropic full matrix least-squares refinement on F^2 for 616 variables converged at $R1 = 0.039$ and $wR2 = 0.096$ with a GOF of 1.09.

Crystals of **6** were grown from vapor diffusion of ether into a methanol solution and mounted on a glass fiber for data collection. X-ray structural analysis for **6** was performed on a $0.47 \times 0.43 \times 0.21 \text{ mm}^3$ blue prism using a 940 frames, twenty second frame ω -scan data collection strategy at 100 K to a $2\theta_{\text{max}} = 58.4^\circ$. **6** crystallizes in the triclinic space group P-1 with unit cell parameters: $a = 8.30645(16) \text{ \AA}$, $b = 12.6697(2) \text{ \AA}$, $c = 13.6657(2) \text{ \AA}$, $\alpha = 93.3069(14)^\circ$, $\beta = 103.0089(16)^\circ$, $\gamma = 107.1032(17)^\circ$, $V = 1327.40(4) \text{ \AA}^3$, $Z = 2$ and $D_{\text{calc}} = 1.707 \text{ Mg/m}^3$. The 7,190 independent data were corrected for absorption (transmission min./max. = 0.745 /1.000; $\mu = 1.078 \text{ mm}^{-1}$). The structure was solved by Patterson methods using SHELX. All non-hydrogen atoms were refined with anisotropic atomic displacement parameters. Methylene, methine, imidazole, amine, methanol and water hydrogen atoms were located by difference maps and refined isotropically. Methyl hydrogen atoms were placed in their geometrically generated positions and refined as a riding model and these atoms were assigned $U(\text{H}) = 1.5 \times U_{\text{eq}}$. For reflections $I > 2\sigma(I)$ ($R(\text{int}) 0.022$) the final anisotropic full matrix least-squares refinement on F^2 for 418 variables converged at $R1 = 0.047$ and $wR2 = 0.105$ with a GOF of 1.05.

Crystals of **7** were grown from vapor diffusion of ether into a methanol solution and mounted on a glass fiber for data collection. X-ray structural analysis for **7** was performed on a $0.42 \times 0.22 \times 0.21 \text{ mm}^3$ blue prism using a 950 frames, twenty second frame ω -scan data collection strategy at 100 K to a $2\theta_{\text{max}} = 57.4^\circ$. **7** crystallizes in the triclinic space group P-1 with unit cell parameters: $a = 7.83639(13) \text{ \AA}$, $b = 11.5417(3) \text{ \AA}$, $c = 12.5358(3) \text{ \AA}$, $\alpha = 88.3240(19)^\circ$, $\beta = 73.9097(18)^\circ$, $\gamma = 82.5500(16)^\circ$, $V = 1080.17(4) \text{ \AA}^3$, $Z = 2$ and $D_{\text{calc}} = 1.677 \text{ Mg/m}^3$. 5,581 independent data were corrected for absorption (transmission min./max. = 0.741 /1.000; $\mu = 1.104 \text{ mm}^{-1}$). The structure was solved by Patterson methods using SHELX. The tetrafluoroborate anion has a tumbling disorder that was modeled with two 50% occupancy groups, (F1a–F6a) and (F1b–F6b) in addition to the full occupancy B atom. To aid in the BF_4 disorder model 42 restraints were used. The ratio for the anion disorder was fixed at 50:50 after being determined from unstable refinement of the F-atom occupancies. All non-hydrogen atoms were refined with anisotropic atomic displacement parameters. Methylene, methine, imidazole, amine, methanol and

water hydrogen atoms were located by difference maps and refined isotropically. Methyl hydrogen atoms were placed in their geometrically generated positions and refined as a riding model and these atoms were assigned $U(H) = 1.5 \times U_{eq}$. For reflections $I > 2\sigma(I)$ ($R(int)$ 0.026) the final anisotropic full matrix least-squares refinement on F^2 for 350 variables converged at $R1 = 0.059$ and $wR2 = 0.126$ with a GOF of 1.05.

Crystals of L_1 were grown from aqueous solution at $4^\circ C$ and mounted on a glass fiber for data collection. X-ray structural analysis for L_1 was performed on a $0.40 \times 0.38 \times 0.33 \text{ mm}^3$ colorless prism using a 900 frames, twenty second frame ω -scan data collection strategy at 100 K to a $2\theta_{max} = 59.1^\circ$. The ligand L_1 crystallizes in the monoclinic space group $C2/c$ with unit cell parameters: $a = 9.37814(17) \text{ \AA}$, $b = 12.2120(2) \text{ \AA}$, $c = 11.9164(2) \text{ \AA}$, $\beta = 95.9045(16)^\circ$, $V = 1357.49(4) \text{ \AA}^3$, $Z = 4$ and $D_{calc} = 1.284 \text{ Mg/m}^3$. The 1,902 independent data were corrected for absorption (transmission min./max. = 0.976/1.000; $\mu = 0.088 \text{ mm}^{-1}$). The structure was solved by Direct methods using SHELX. All non-hydrogen atoms were refined with anisotropic atomic displacement parameters. Methylene, methine, imidazole and water hydrogen atoms were located by difference maps and refined isotropically. Methyl hydrogen atoms were placed in their geometrically generated positions and their thermal parameters were allowed to refine. For reflections $I > 2\sigma(I)$ ($R(int)$ 0.019) the final anisotropic full matrix least-squares refinement on F^2 for 115 variables converged at $R1 = 0.034$ and $wR2 = 0.082$ with a GOF of 1.04.

References

1. CrysAlis PRO (CCD and RED), V 1.171.36.32, Agilent Technologies (2013).
2. SCALE3 ABSPACK included in CrysAlis PRO RED, V 1.171.36.32.
3. G. M. Sheldrick. *Acta Crystallogr.* 2008, *A64*, 112-122. (SHELX)
4. ORTEP-3 for Windows, L. J. Farrugia, *J. Appl. Crystallogr.* 1997, **30**, 565.

Table S1. Crystal Data and Structure Refinement for **1,4 – 7**, and **L₁**.

	1	4	5	6	7	L₁
	C ₁₄ H ₁₉ Cl ₂ CuN ₇ O ₈	C ₁₂ H ₁₈ Cl ₂ CuN ₆ O ₉	C ₁₄ H ₂₄ Cl ₂ CuN ₆ O ₁₀	C ₁₆ H ₂₄ CuF ₆ N ₆ O ₈ S· 0.67H ₂ O	C ₁₄ H ₂₄ B ₂ CuF ₈ N ₆ O ₂	C ₁₂ H ₁₈ N ₆ O
empirical formula						
formula weight	547.80	524.76	570.83	682.15	545.55	262.32
temperature (K)	100.1(3)	100.1(10)	100.1(6)	100.0(6)	100.2(4)	99.95(10)
wavelength (Å)	0.71073	0.71073	0.71073	0.71073	0.71073	0.71073
crystal system	triclinic	triclinic	monoclinic	triclinic	triclinic	monoclinic
space group	<i>P</i> -1	<i>P</i> -1	<i>Pn</i>	<i>P</i> -1	<i>P</i> -1	<i>C2/c</i>
unit cell dimensions						
<i>a</i> (Å)	8.7479(8)	8.227(3)	13.0049(3)	8.30645(16)	7.83639(13)	9.37814(17)
<i>b</i> (Å)	10.1421(7)	11.003(4)	11.5913(2)	12.6697(2)	11.5417(3)	12.2120(2)
<i>c</i> (Å)	12.9690(10)	11.441(4)	15.1039(4)	13.6657(2)	12.5358(3)	11.9164(2)
α (°)	68.941(7)	78.99(3)		93.3069(14)	88.3240(19)	
β (°)	75.950(7)	70.69(3)	104.371(3)	103.0089(16)	73.9097(18)	95.9045(16)
γ (°)	88.025(7)	88.76(3)		107.1032(17)	82.5500(16)	
volume (Å ³)	1039.90(14)	958.5(6)	2205.57(9)	1327.40(4)	1080.17(4)	1357.49(4)
<i>Z</i>	2	2	4	2	2	4
density (Mg/m ³) (calcd)	1.749	1.818	1.719	1.707	1.677	1.284
abs. coefficient (mm ⁻¹)	1.367	1.481	1.298	1.078	1.104	0.088
crystal size (mm ³)	0.42 × 0.40 × 0.03	0.28 × 0.21 × 0.02	0.35 × 0.28 × 0.2	0.47 × 0.43 × 0.2	0.42 × 0.22 × 0.2	0.40 × 0.38 × 0.3
crystal color, habit	3	2	6	1	1	3
θ range for data coll. (°)	blue plate	light blue plate	blue prism	blue prism	blue prism	colorless prism
	3.22 – 28.68	3.30 – 27.68	3.29 – 28.16	3.32 – 29.20	3.44 – 28.69	3.34 – 29.56
	-11 ≤ <i>h</i> ≤ 11	-10 ≤ <i>h</i> ≤ 10	-17 ≤ <i>h</i> ≤ 17	-11 ≤ <i>h</i> ≤ 11	-10 ≤ <i>h</i> ≤ 10	-12 ≤ <i>h</i> ≤ 12
	-13 ≤ <i>k</i> ≤ 13	-14 ≤ <i>k</i> ≤ 14	-15 ≤ <i>k</i> ≤ 15	-17 ≤ <i>k</i> ≤ 17	-15 ≤ <i>k</i> ≤ 15	-16 ≤ <i>k</i> ≤ 16
	-17 ≤ <i>l</i> ≤ 17	-14 ≤ <i>l</i> ≤ 14	-20 ≤ <i>l</i> ≤ 20	-18 ≤ <i>l</i> ≤ 18	-16 ≤ <i>l</i> ≤ 16	-15 ≤ <i>l</i> ≤ 16
index ranges						
reflections collected	42429	19076	83528	34182	27089	16814
	5359	4447	10813	7190	5581	1902
independent reflections	[<i>R</i> (int) = 0.050]	[<i>R</i> (int) = 0.043]	[<i>R</i> (int) = 0.041]	[<i>R</i> (int) = 0.022]	[<i>R</i> (int) = 0.026]	[<i>R</i> (int) = 0.0190]
completeness to θ max	99.7	99.3	99.8	99.7	99.8	99.6
absorption correction				multi-scan		
min. and max. trans.	0.63 and 1.00	0.038 and 1.00	0.81 and 1.00	0.75 and 1.00	0.074 and 1.00	0.98 and 1.00
refinement method				full-matrix least squares on <i>F</i> ²		
data/restraints/parameters	5359/0/332	4447/0/317	10813/4/616	7190/3/418	5581/42/350	1902/0/115
GOF on <i>F</i> ²	1.041	1.063	1.097	1.047	1.048	1.038
final <i>R</i> indices [<i>I</i> > 2 σ (<i>I</i>)] ^{a,b}	<i>R</i> 1 = 0.0350, w <i>R</i> 2 = 0.0861	<i>R</i> 1 = 0.0458, w <i>R</i> 2 = 0.1193	<i>R</i> 1 = 0.0396, w <i>R</i> 2 = 0.0961	<i>R</i> 1 = 0.0471, w <i>R</i> 2 = 0.1047	<i>R</i> 1 = 0.0594, w <i>R</i> 2 = 0.1257	<i>R</i> 1 = 0.0341, w <i>R</i> 2 = 0.0822
	<i>R</i> 1 = 0.0382, w <i>R</i> 2 = 0.00892	<i>R</i> 1 = 0.0541, w <i>R</i> 2 = 0.1270	<i>R</i> 1 = 0.0415, w <i>R</i> 2 = 0.0979	<i>R</i> 1 = 0.0506, w <i>R</i> 2 = 0.1065	<i>R</i> 1 = 0.0645, w <i>R</i> 2 = 0.1288	<i>R</i> 1 = 0.0368, w <i>R</i> 2 = 0.0840
<i>R</i> indices (all data) ^{a,b}						
largest peak and hole (e·Å ⁻³)	0.958 and -0.407	1.320 and -0.559	1.847 and -0.370	1.718 and -0.974	2.793 and -1.901	0.303 and -0.258

^a*R*1 = $\sum ||F_o| - |F_c|| / \sum |F_o|$; ^bw*R*2 = $\{\sum [w(F_o^2 - F_c^2)^2] / \sum [w(F_o^2)^2]\}^{1/2}$; where $w = q / \sigma^2(F_o^2) + (qp)^2 + bp$.

GOF = $S = \{\sum [w(F_o^2 - F_c^2)^2] / (n - p)\}^{1/2}$.

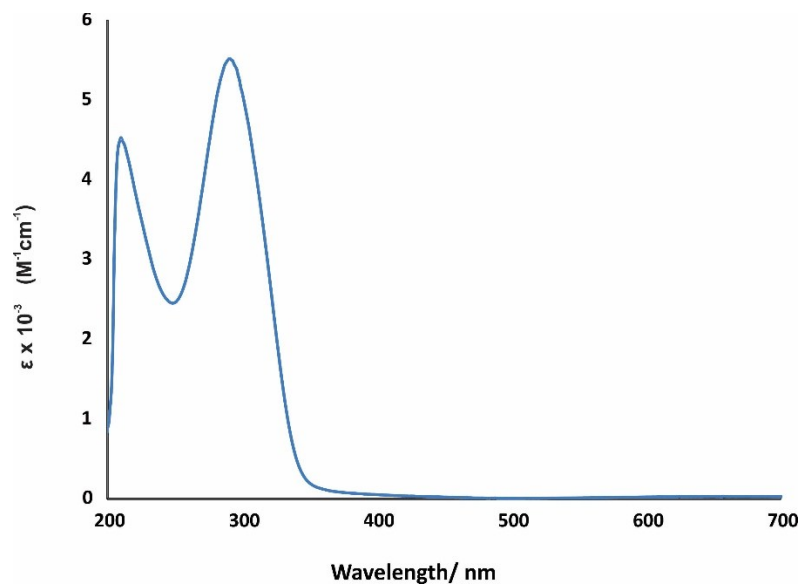


Figure S1. Electronic spectrum of **2** in acetonitrile.

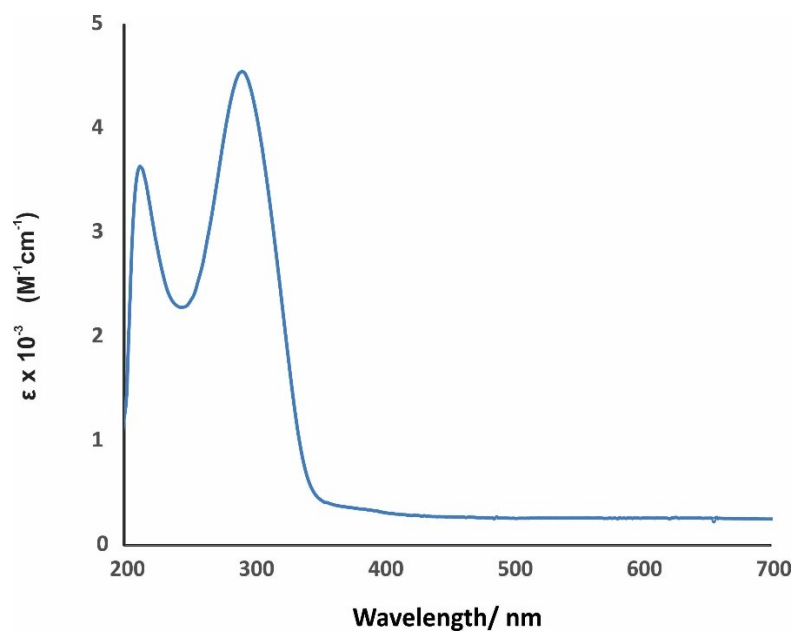


Figure S2. Electronic spectrum of **3** in acetonitrile.

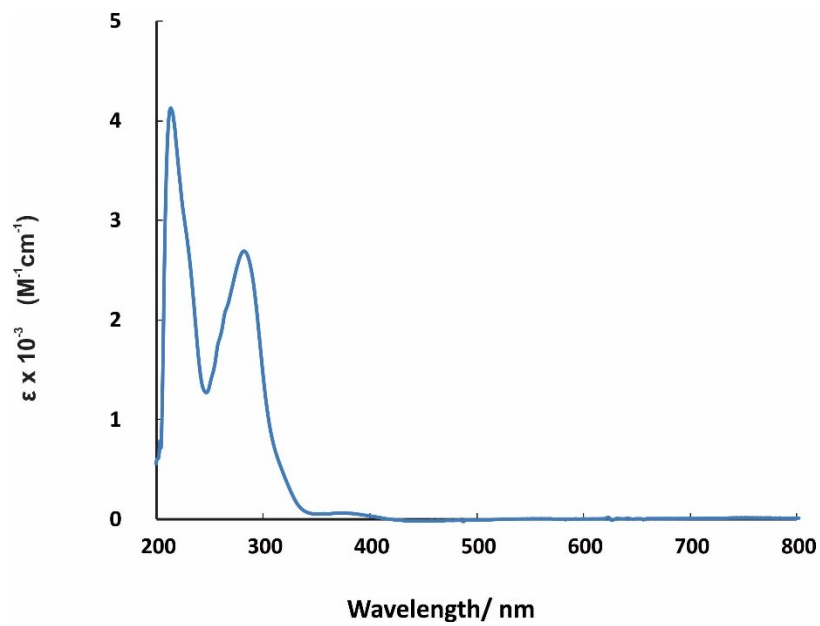


Figure S3. Electronic spectrum of **6** in acetonitrile.

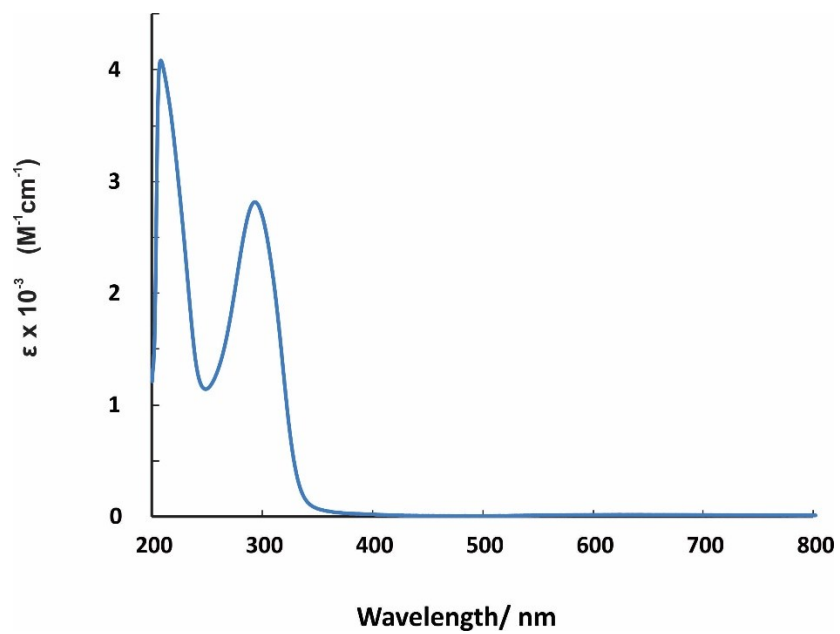


Figure S4. Electronic spectrum of **7** in acetonitrile.

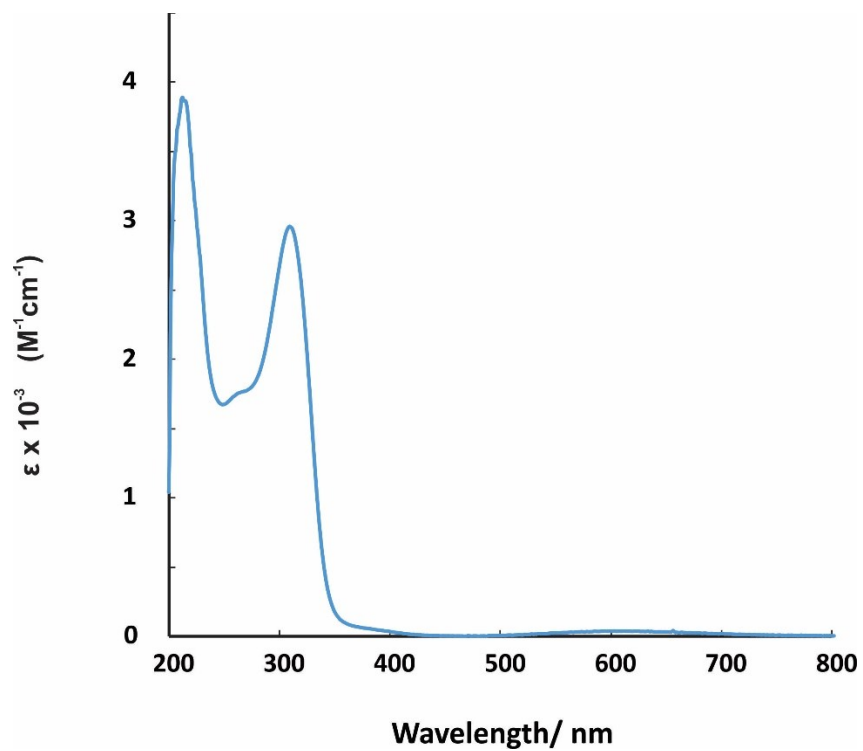


Figure S5. Electronic spectrum of **8** in acetonitrile (non-dried).

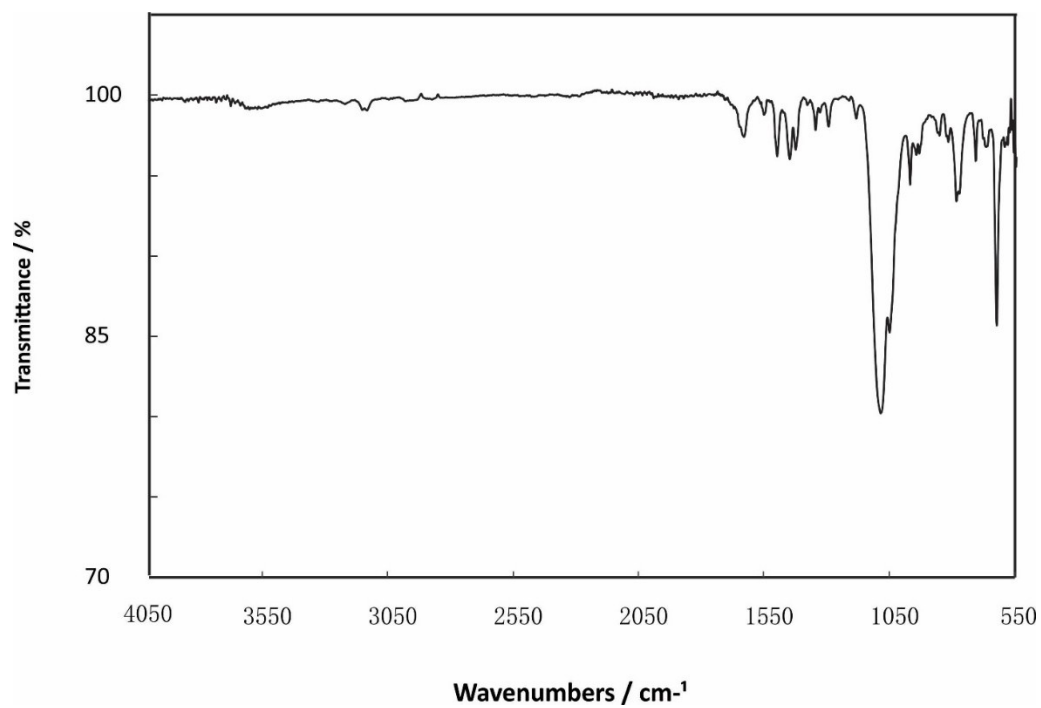


Figure S6. IR spectrum of **1**.

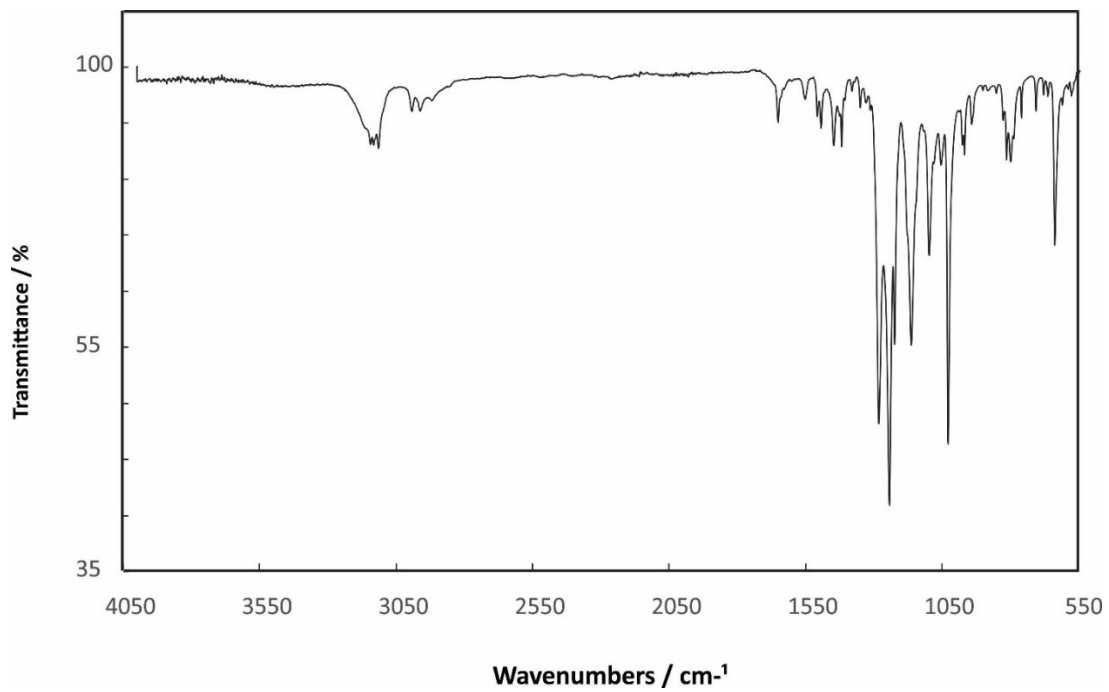


Figure S7. IR spectrum of **2**.

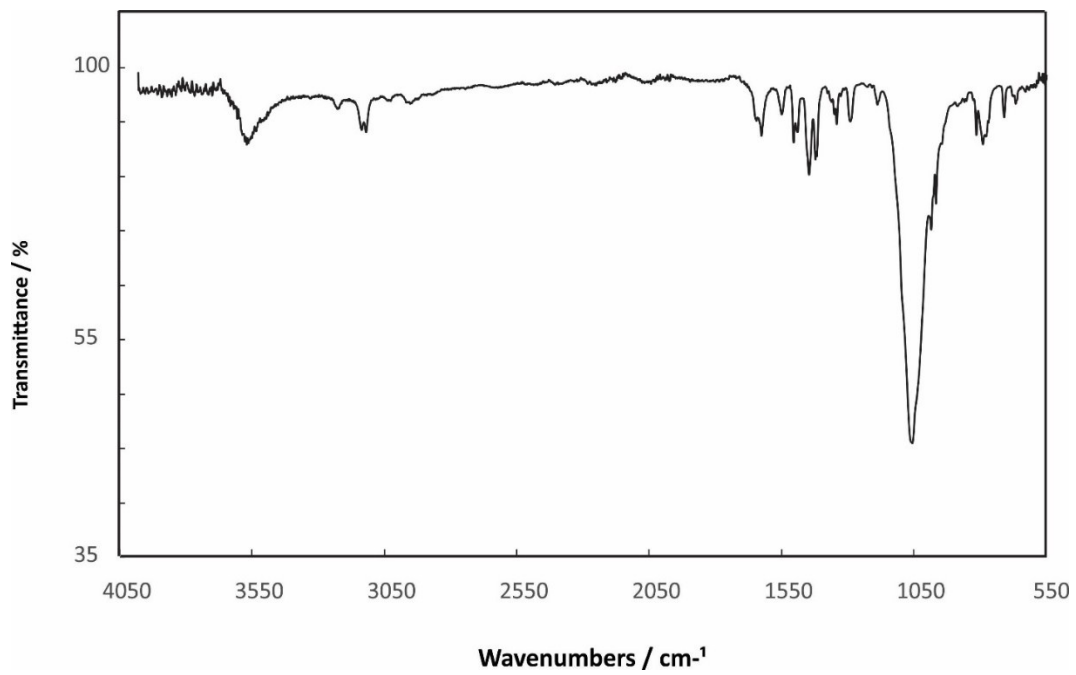


Figure S8. IR spectrum of **3**.

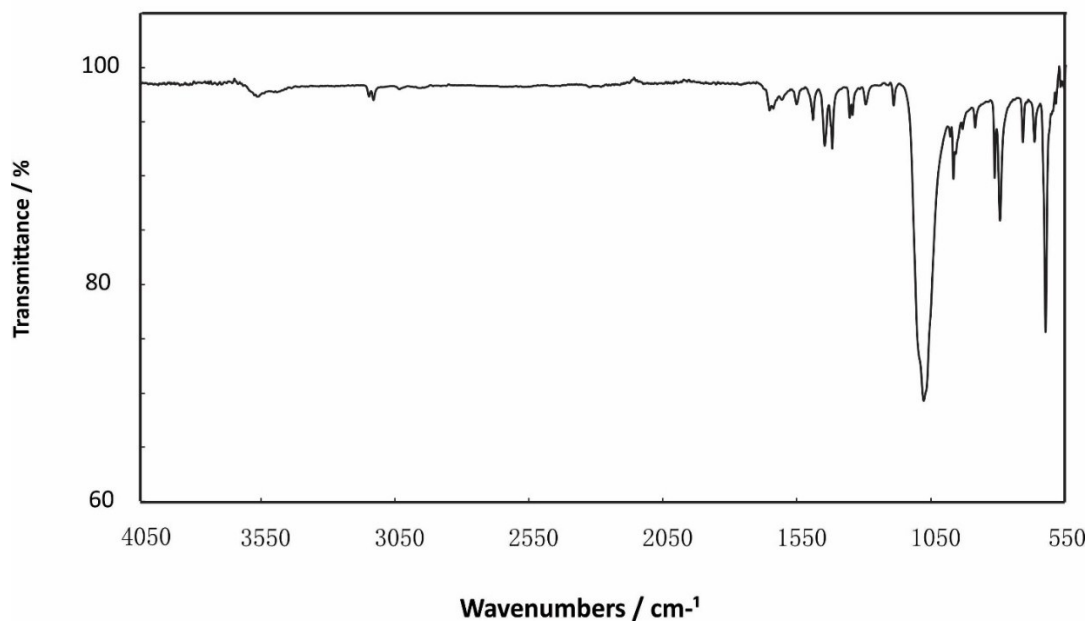


Figure S9. IR spectrum of 4.

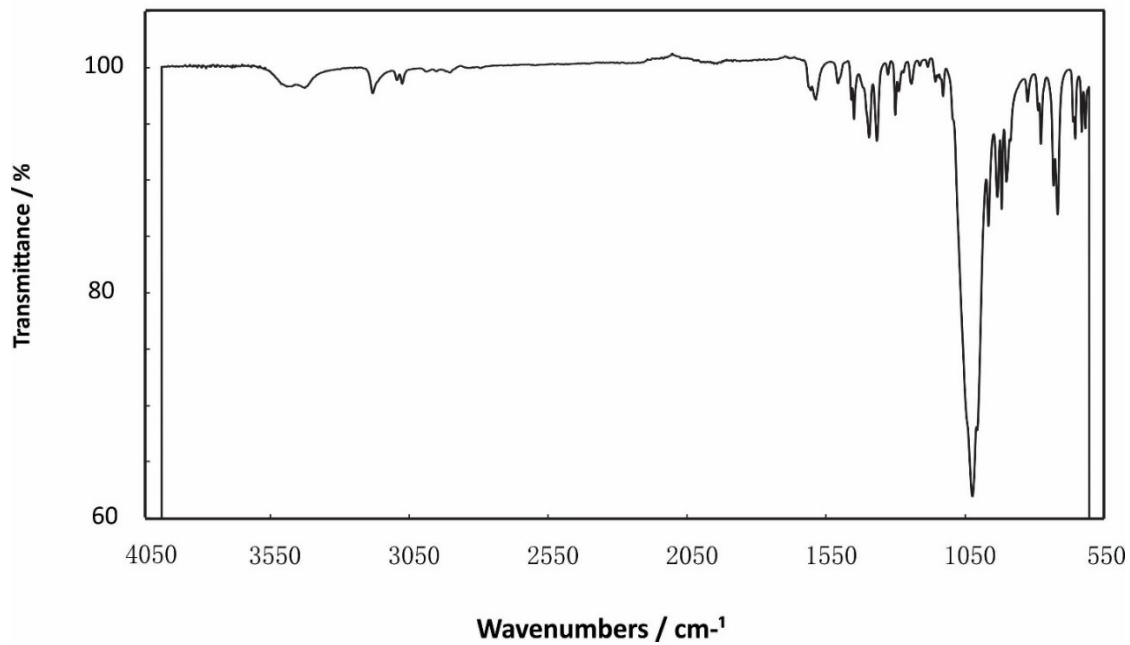


Figure S10. IR spectrum of 5.

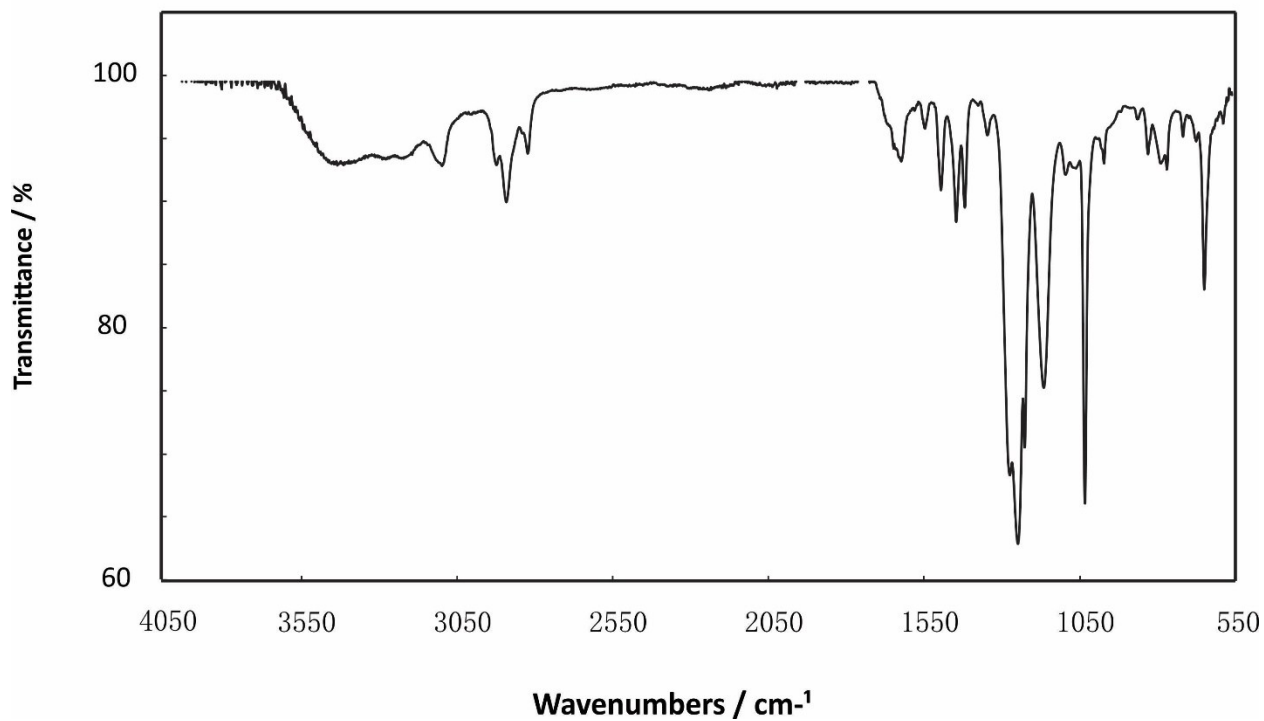


Figure S11. IR spectrum of **6**.

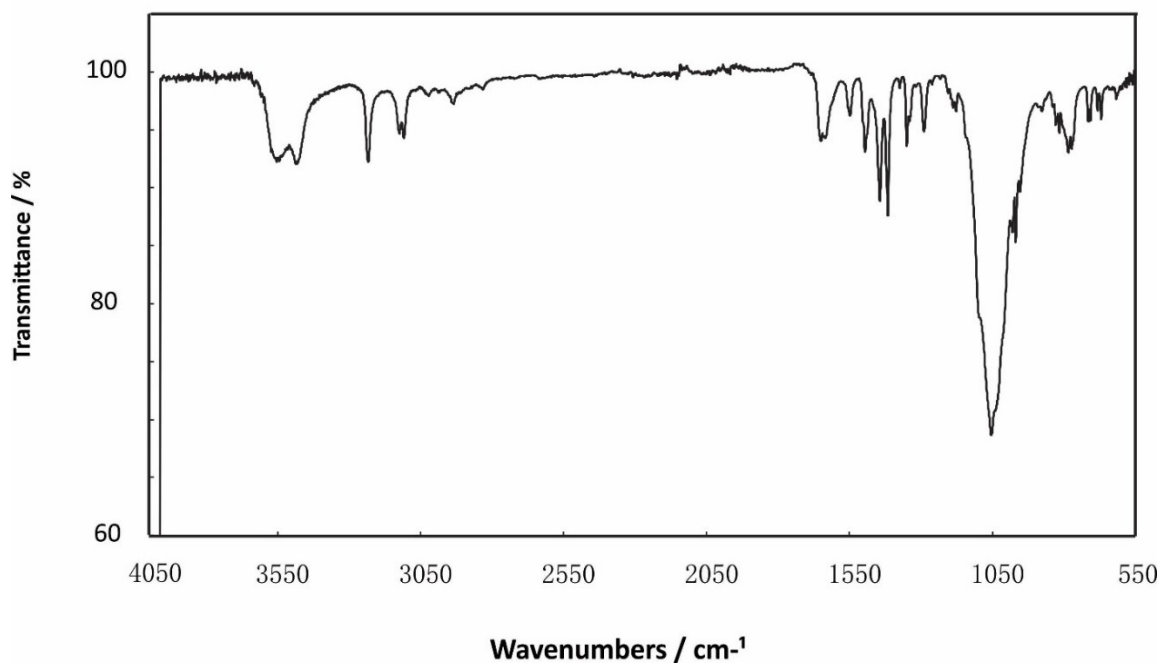


Figure S12. IR spectrum of **7**.

+TOF MS: 0.017 to 0.500 min from 04221503p.wiff
a=3.56446222539229020e-004, t0=-1.43464231559846670e+001 R;

Max. 1225.3 counts.

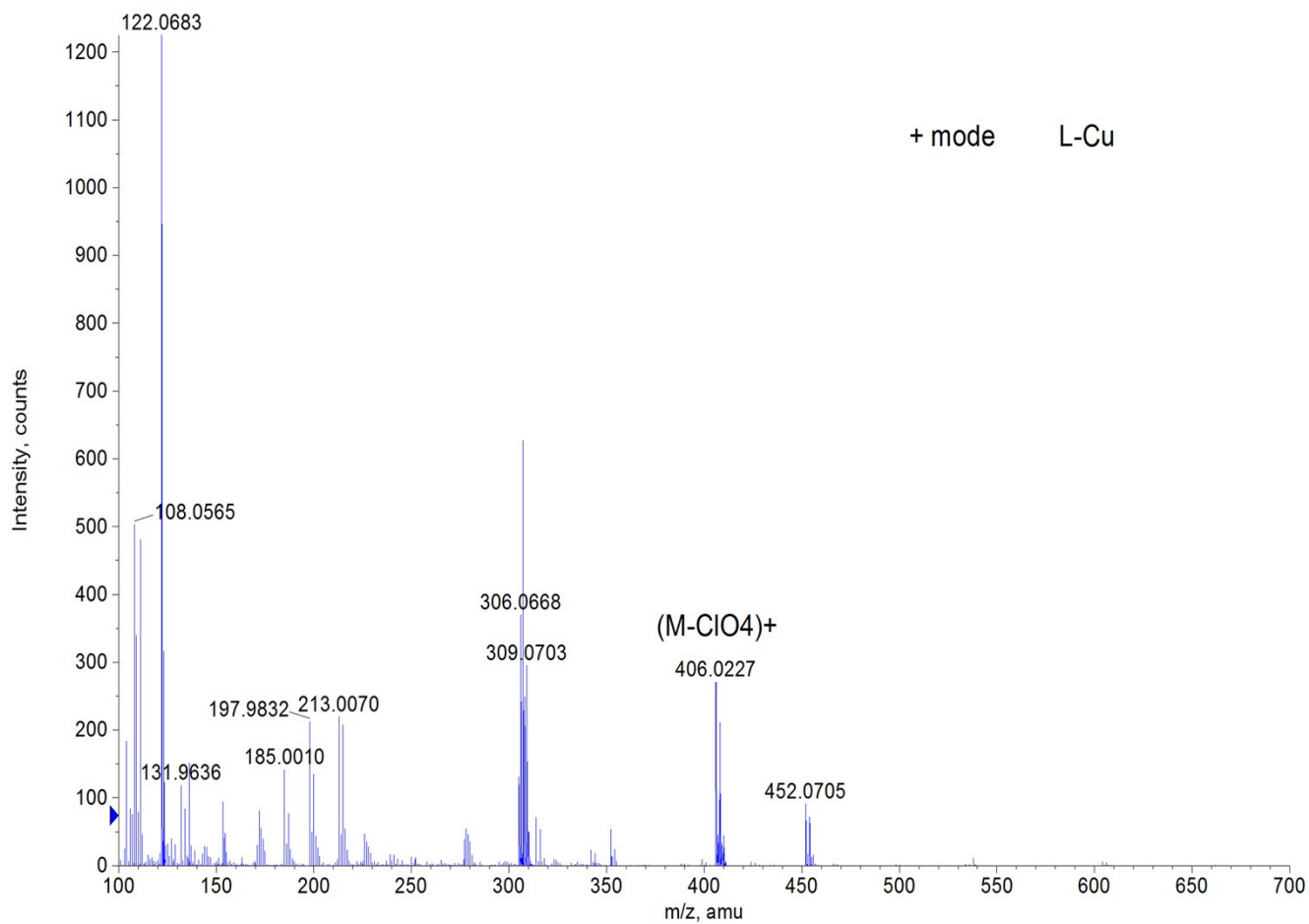


Figure S13. +ESI spectrum of 1.

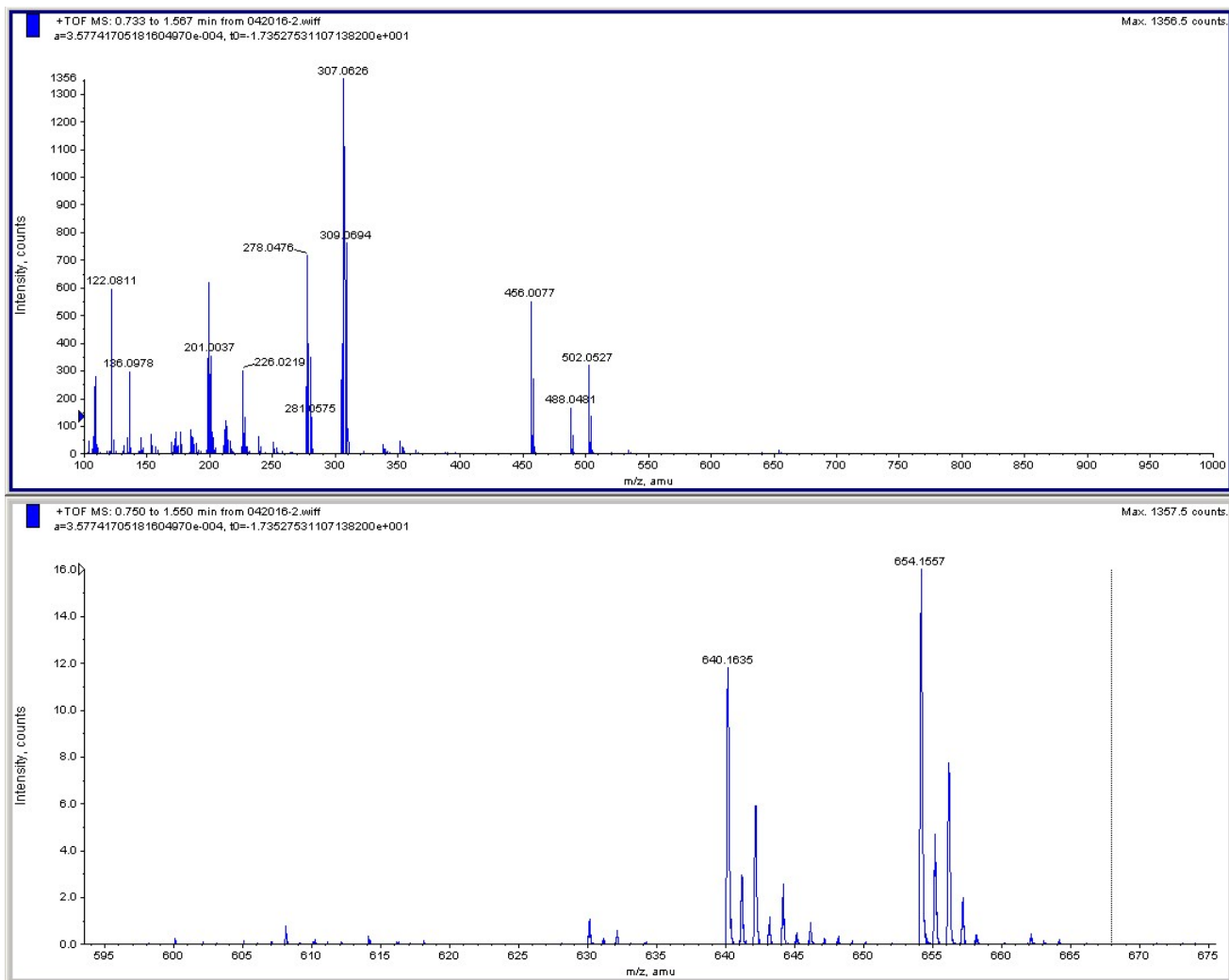


Figure S14. +ESI spectrum of 2.

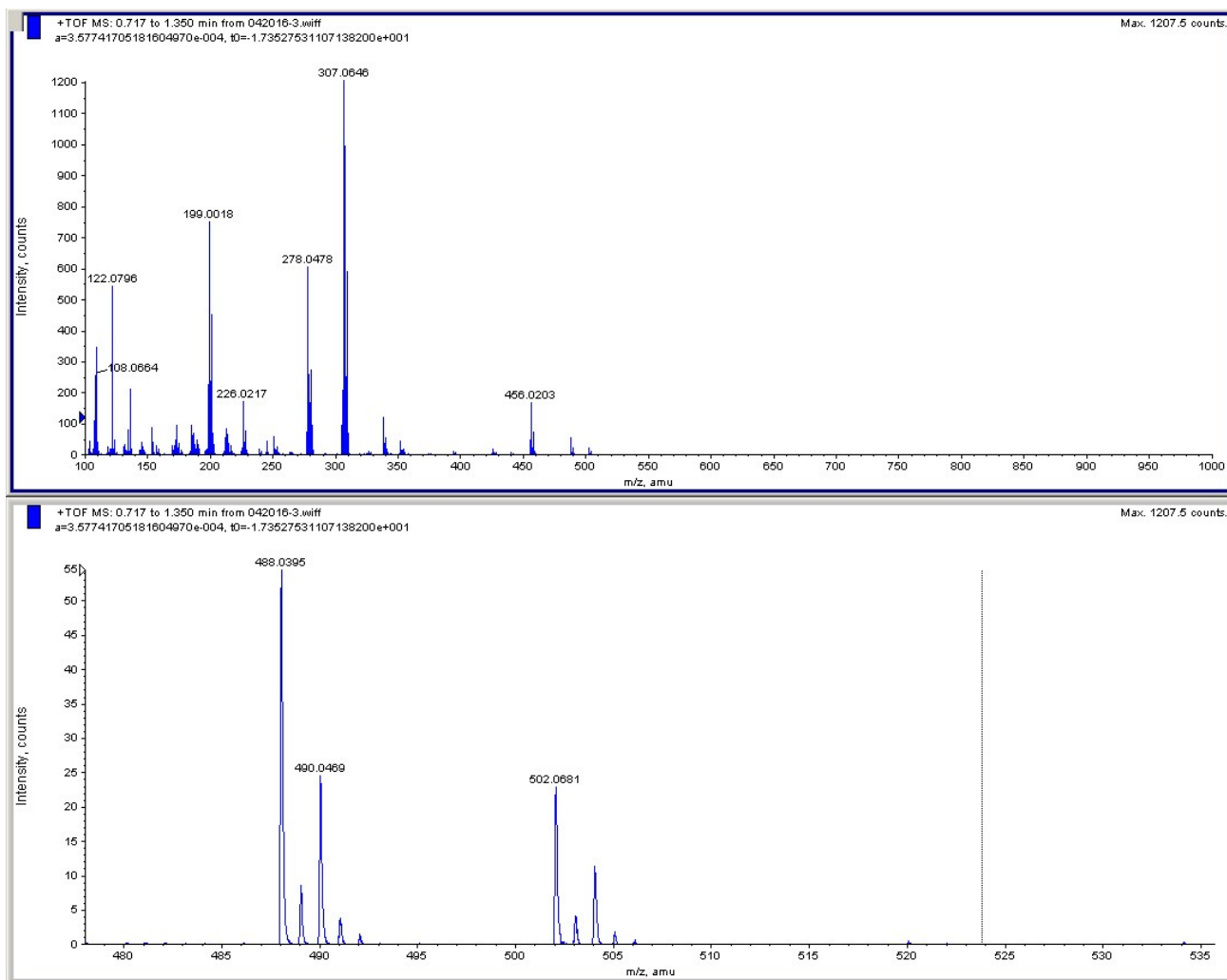


Figure S15. +ESI spectrum of 3.

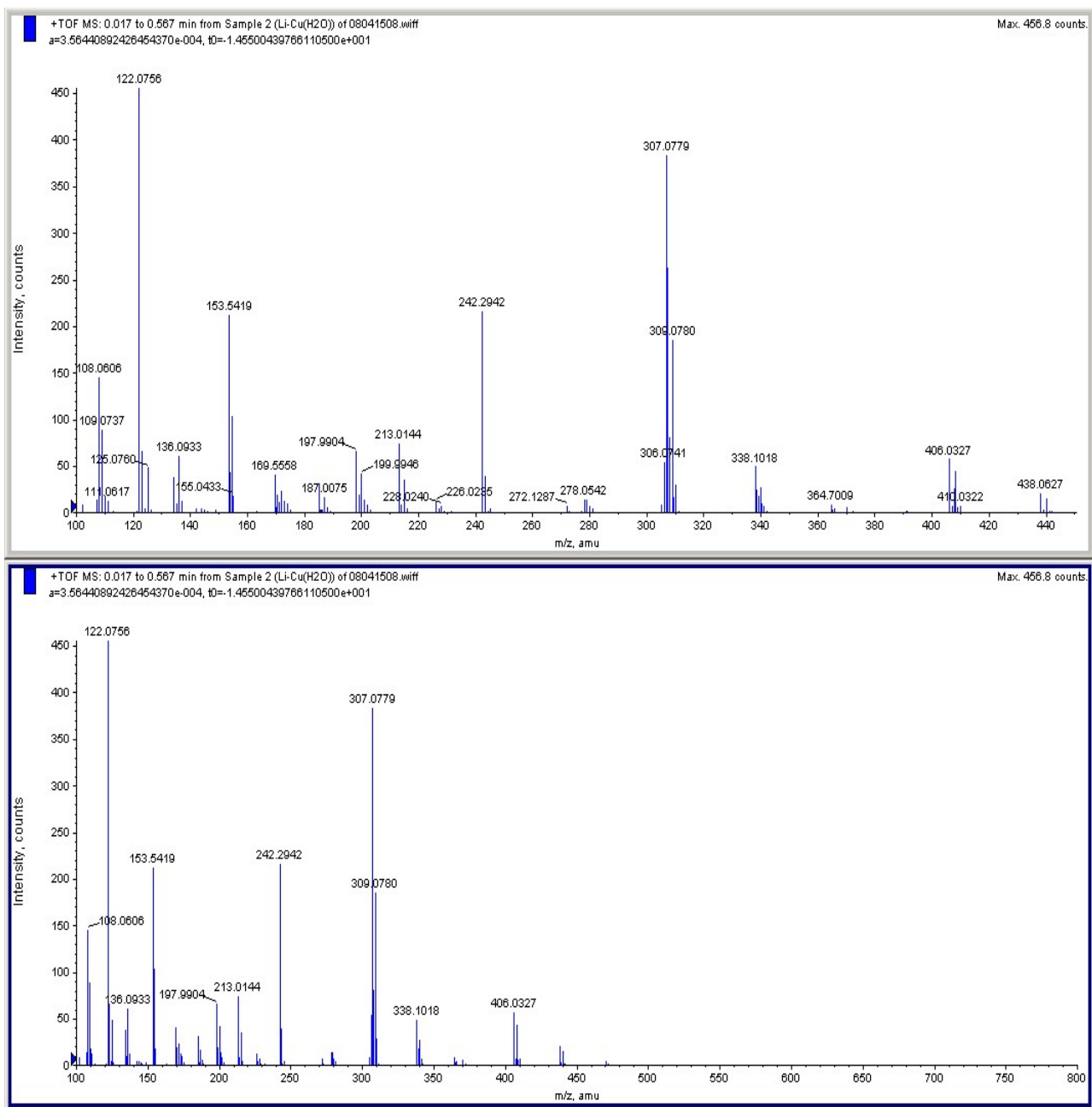


Figure S16. +ESI spectrum of 4.

+TOF MS: 0.017 to 0.500 min from Sample 2 (l3-cu) of 04221502p.wiff
a=3.56445771037246140e-004, t0=-1.43464231559846670e+001

Max. 1507.9 counts.

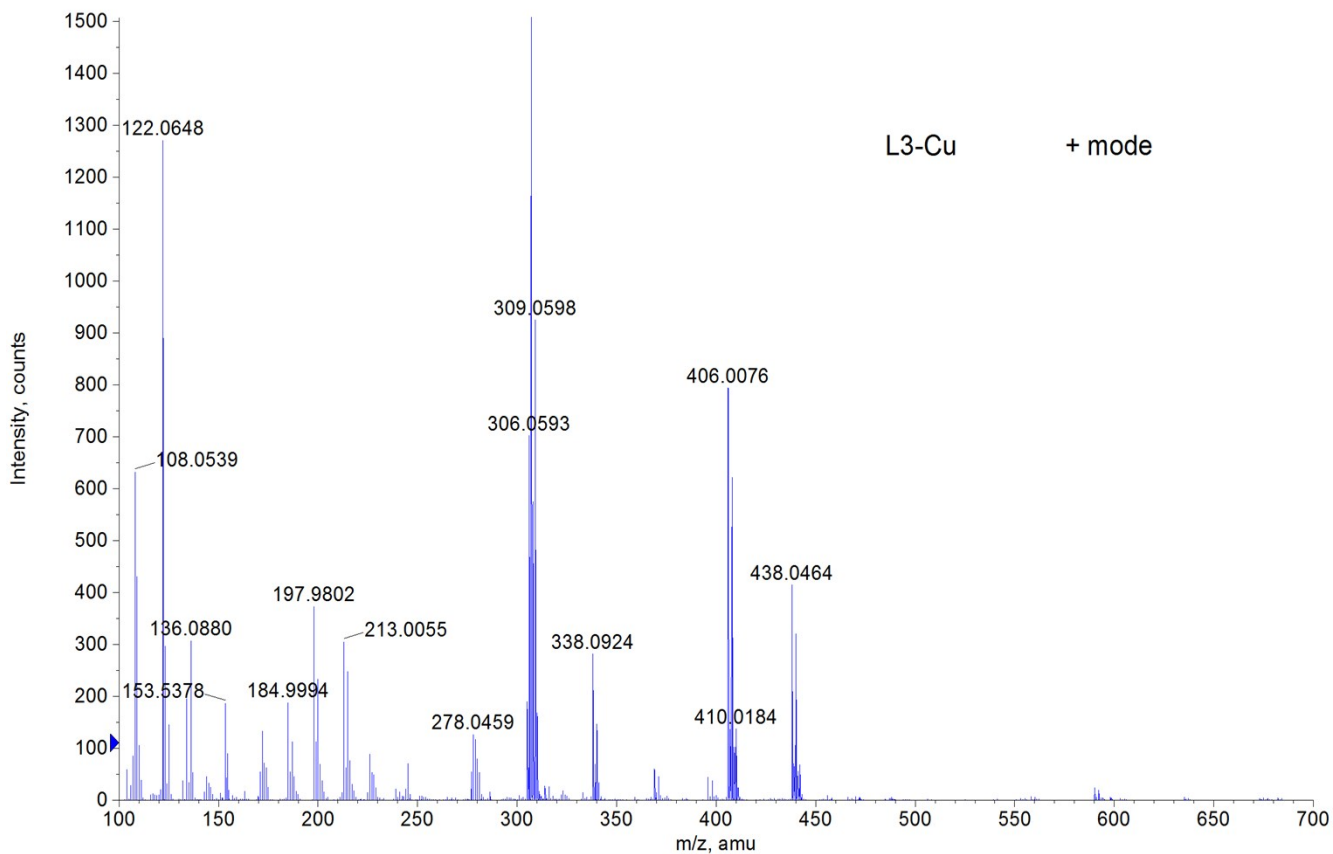


Figure S17. +ESI spectrum of 5.

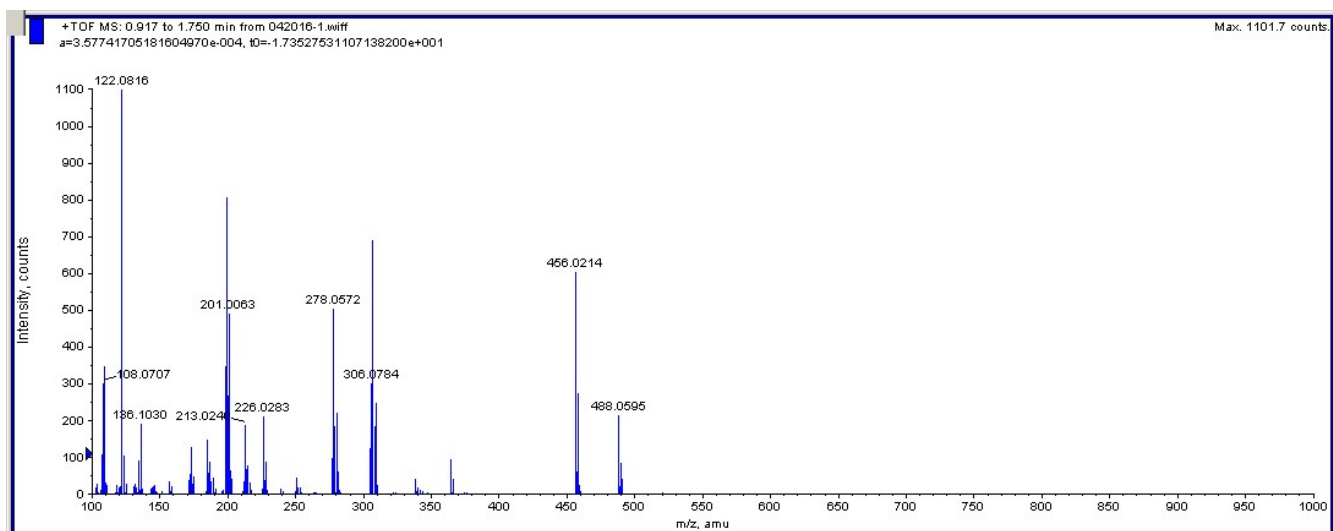


Figure S18. +ESI spectrum of 6.

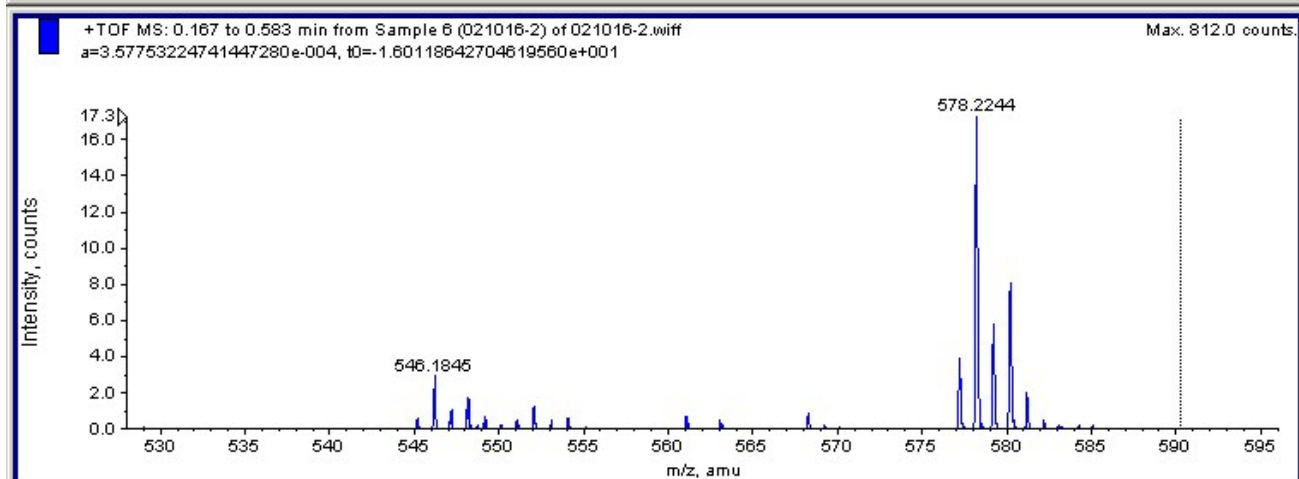
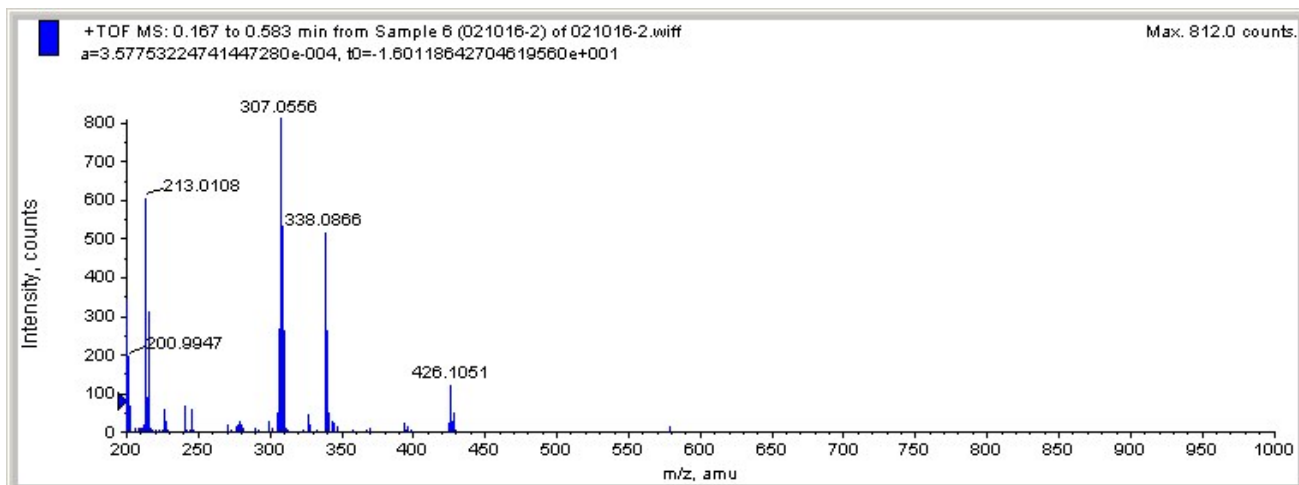


Figure S19. +ESI spectrum of 7.

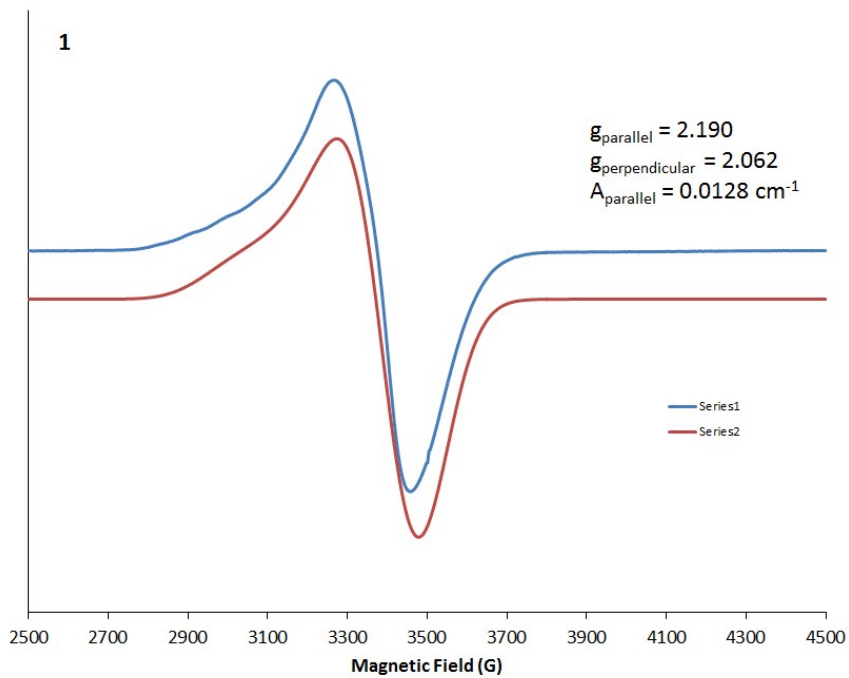


Figure S20. Experimental and simulated room temperature powder EPR spectrum of **1**.

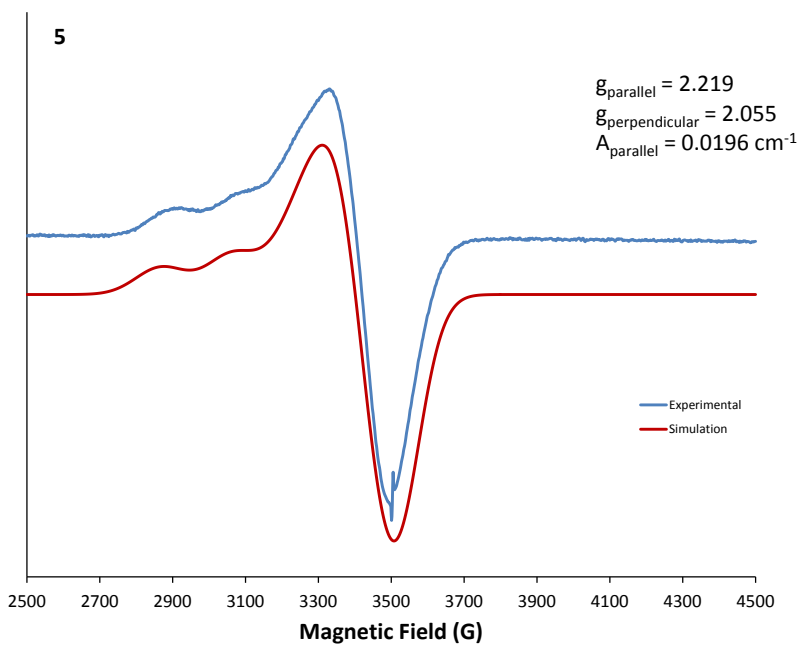


Figure S21. Experimental and simulated room temperature powder EPR spectrum of **5**. The small feature near $B = 3500$ G is an impurity in the EPR tube.

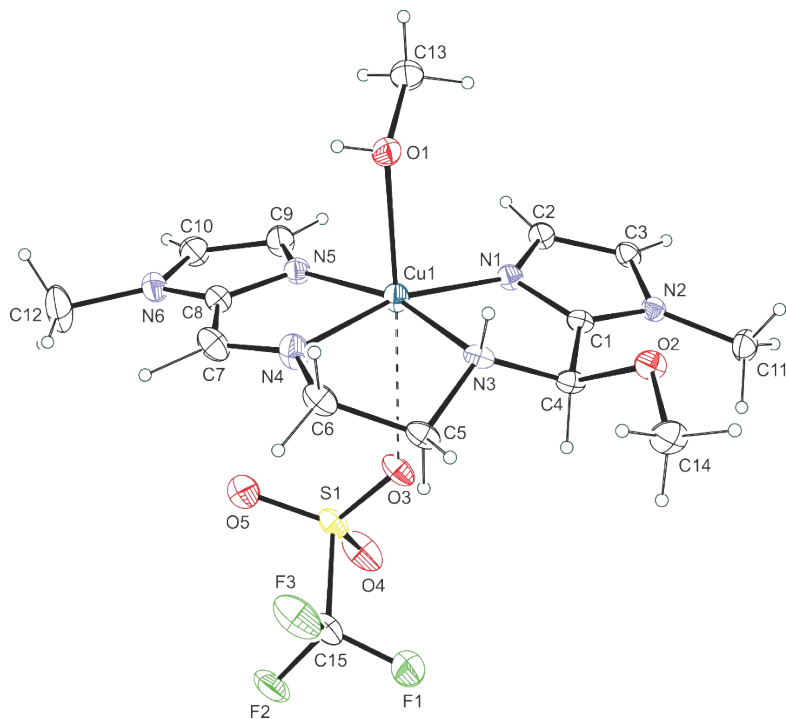


Figure S22. ORTEP⁴ representation of $\{[L_2-Cu(CH_3OH)] \cdot OTf\}^+$ of **6**.

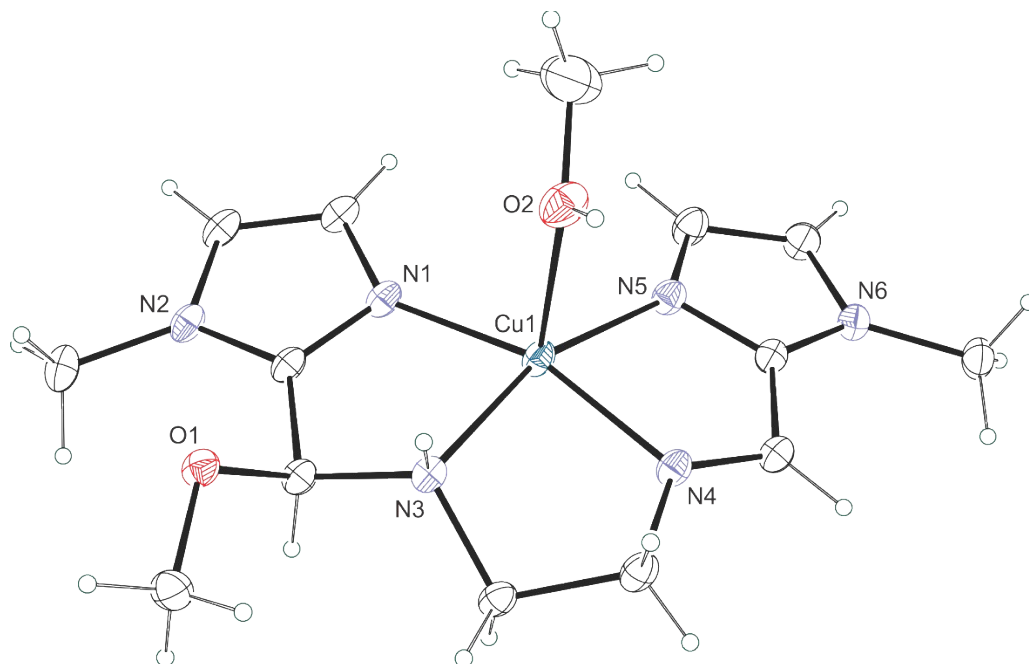


Figure S23. ORTEP⁴ representation of $[L_2-Cu(CH_3OH)]^{2+}$ of **7**.

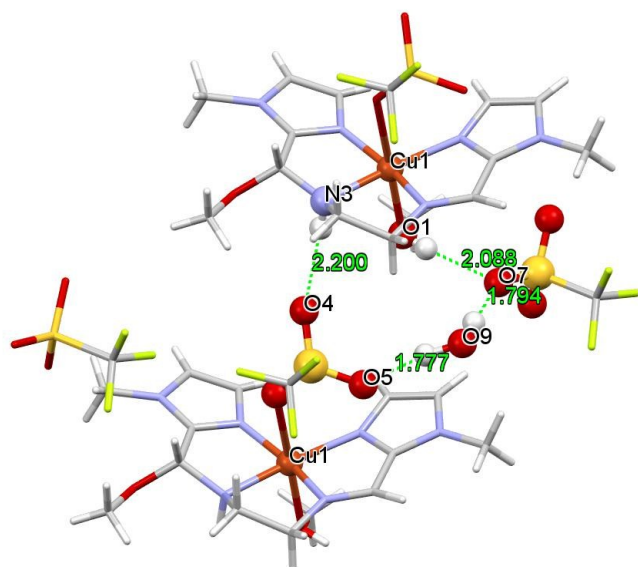


Figure S24. Non-covalent interactions in **6**. Hydrogen bond D...A acceptor distances are indicated in units of Å.

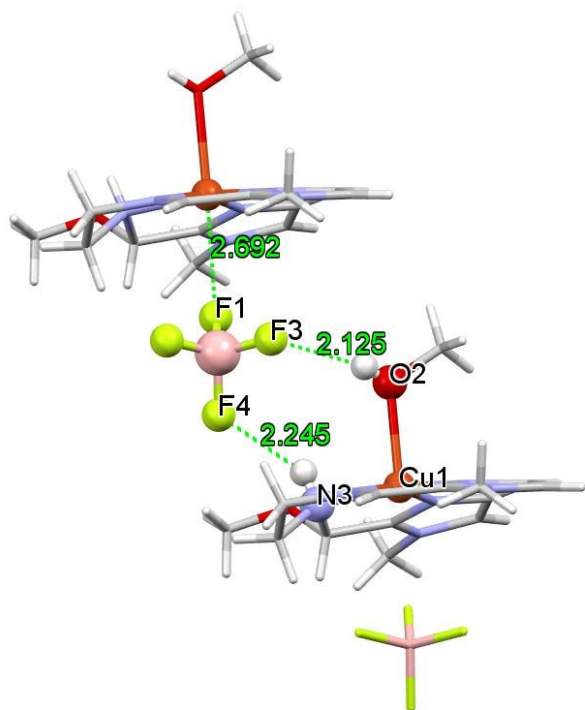


Figure S25. Non-covalent interactions in **7**. Hydrogen bond D...A acceptor distances are indicated in units of Å.

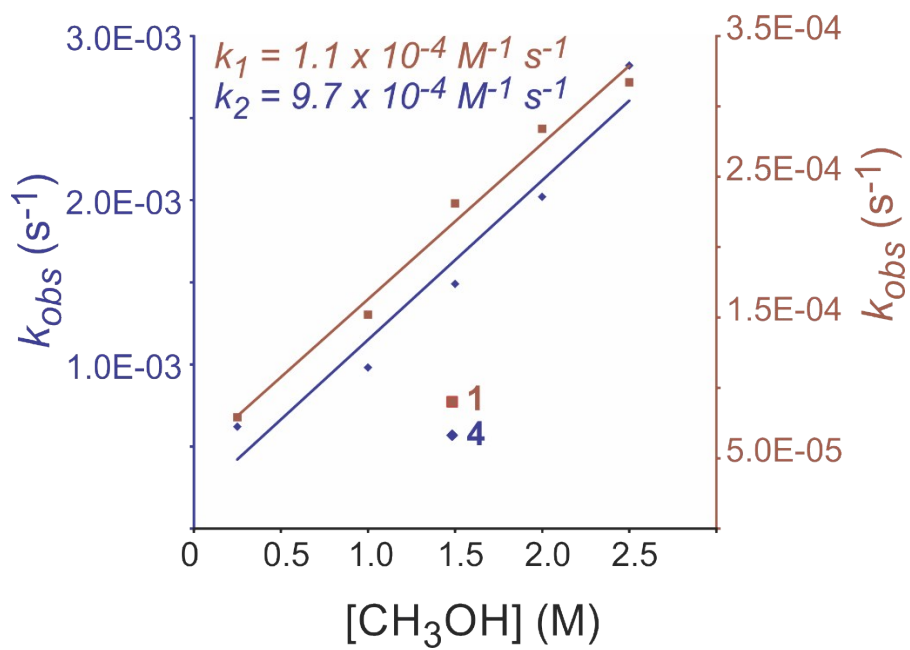


Figure S26. Plot of k_{obs} versus $[\text{CH}_3\text{OH}]$ for **1** and **4**.

Figure X. Plot of k_{obs} versus $[\text{CH}_3\text{OH}]$ for **1** and **4**.

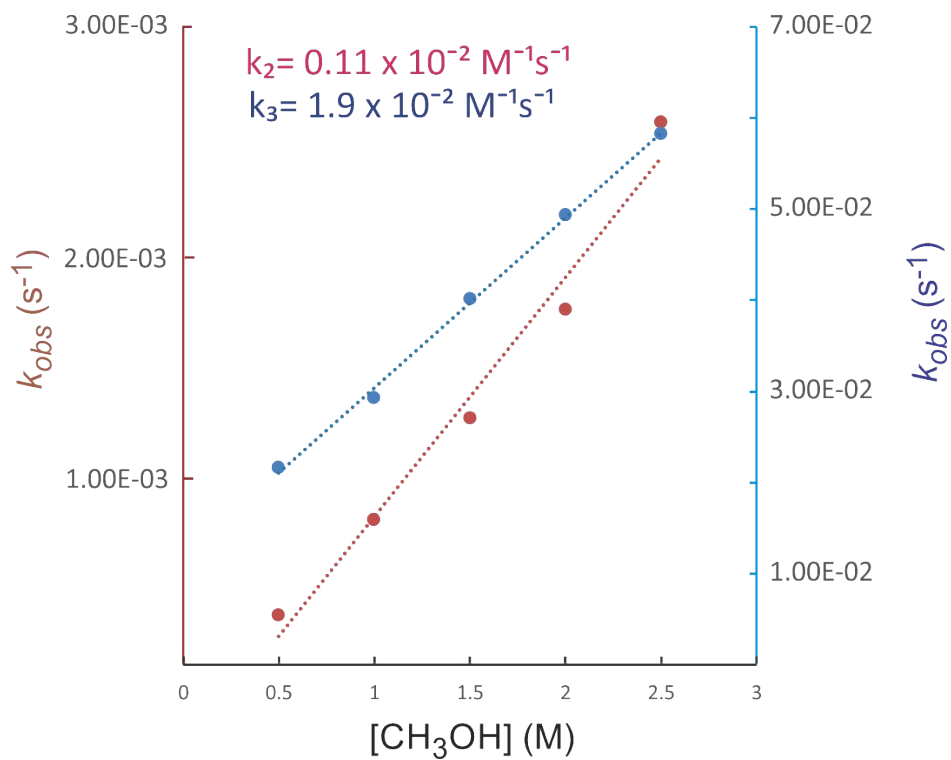


Figure S27. Plot of k_{obs} versus $[\text{CH}_3\text{OH}]$ for **2** and **3**.